The *Arabidopsis* double-stranded RNA-binding protein HYL1 plays a role in microRNA-mediated gene regulation

Meng-Hsuan Han, Saiprasad Goud, Liang Song, and Nina Fedoroff*

Biology Department and Huck Institutes of Life Sciences, Pennsylvania State University, University Park, PA 16802

Contributed by Nina Fedoroff, December 2, 2003

The *Arabidopsis HYL1* gene encodes a nuclear double-stranded RNA-binding protein. A knockout mutation of the *hyl1* gene is recessive and pleiotropic, causing developmental abnormalities, increasing sensitivity to abscisic acid, and reducing sensitivity to auxin and cytokinin. We report that levels of several microRNAs (miRNAs; miR159, -167, and -171) are reduced in homozygous mutant plants, and levels of two of three tested target mRNAs are elevated. Conversely, the miRNA levels are elevated in plants expressing a *HYL1* cDNA from a strong promoter, and the corresponding target RNAs are reduced. These changes result from alterations in the stability of the target RNAs. However, double-stranded RNA-induced posttranscriptional gene silencing is unaffected by the *hyl1* mutation. One-third to one-half of the cellular HYL1 protein is in a macromolecular complex, and a GFP-HYL1 fusion protein is found predominantly in the nucleus, although it is observed in both nucleus and cytoplasm in some cells. Within nuclei, HYL1 is associated with subnuclear bodies and ring-like structures. These observations provide evidence that the HYL1 protein is part of a nuclear macromolecular complex that is involved in miRNA-mediated gene regulation. Because *hyl1* mutants show marked abnormalities in hormone responses, these results further suggest that miRNA-mediated changes in mRNA stability play a vital role in plant hormone signaling.

Recent studies on gene silencing have uncovered highly selective RNA-based mechanisms that inhibit gene expression by interfering with mRNA translation or enhancing mRNA degradation (1–3). These gene-silencing mechanisms, commonly termed RNA interference in animals and posttranscriptional gene silencing (PTGS) in plants, derive their gene specificity from short, initially double-stranded RNAs (dsRNAs) with extensive homology with or identity to the mRNA targets. Endogenous gene expression is controlled by similar mechanisms in microorganisms, plants, and animals through a family of tiny RNAs termed microRNAs (miRNAs) (4, 5). The discovery that miRNAs can be developmental regulators has defined a new and exciting area of regulatory biology (6–8).

miRNAs are endogenous, single-stranded ≈21-nt RNAs that are produced from noncoding hairpin-containing precursors varying in length from ≈70 to >300 nt (6, 9–15). These small RNAs are processed by RNase III-like proteins, including the human nuclear protein Drosha, the cytoplasmic protein DICER in animals, and the plant nuclear protein DICER-LIKE 1 (DCL1) (16–20). An additional previously undescribed protein, the HUA ENHANCER 1 (HEN1) protein, participates in producing both miRNA and the short interfering RNAs involved in PTGS by sense transcripts in *Arabidopsis* (14, 21). miRNAs can regulate target mRNAs by either translational repression or RNA cleavage in both animals and plants, depending on the degree of complementarity between the miRNA and its target (5, 8, 22–24). The recent finding that miR172 in *Arabidopsis* regulates both the translation and the stability of its target mRNA, albeit to different extents, suggests that a single miRNA can effect both translational silencing and mRNA degradation (8).

Evidence is accumulating rapidly that miRNAs play key roles in gene regulation and development in both animals and plants. The *lin-4* and *let-7* miRNAs in *Caenorhabditis elegans* act as antisense translational repressors by imperfect complementarity to the 3′ UTR of their target mRNAs (25–27). The temporal pattern of miRNA expression controls developmental timing during the larval stage. Indeed, many other miRNAs in both animals and plants accumulate in a temporally or spatially restricted manner, consistent with a regulatory function in development (6, 9–11, 14, 28). In plants, the miRNA miR-JAW triggers cleavage of several *TCP* mRNAs in leaf development (7), whereas miR172 regulates flowering time and floral organ identity by down-regulating *AP2*-like target genes (8, 23). Mutations that alter miRNA metabolism are pleiotropic (14, 16). Both *dcl1* and *hen1* mutant plants exhibit a wide array of developmental defects, including altered leaf shape and reduced plant height, carpel fusion, and female fertility. P1/HC-Pro, a viral suppressor of RNA silencing which interferes with miRNA function, also produces defects resembling those in *dcl1* and *hen1* mutant plants (29).

We have described a recessive *Ds* transposon insertion mutation, designated *hyponastic leaves 1* (*hyl1*), in a gene coding for a nuclear dsRNA-binding protein (30). The mutation is pleiotropic, resulting in reduced leaf size and severe leaf hyponasty, slow growth and reduced plant height, late flowering and reduced fertility, as well as multiple lateral shoots, giving a bushy phenotype. Homozygous *hyl1* mutant plants exhibit reduced sensitivity to exogenous cytokinin and auxin, as well as additional auxin phenotypes that include reduced root gravitropism and apical dominance. By contrast, the *hyl1* mutant is hypersensitive to germination inhibition by abscisic acid (30, 31), and it is also hypersensitive to glucose, NaCl, and osmotic stress (C. Lu and N.F., unpublished data) but has normal responses to other hormones.

The HYL1 protein has two dsRNA-binding domains in its N-terminal half and preferentially binds dsRNA *in vitro* (30). Among the closest homologs of the N-terminal half of the protein are the RDE-4 protein of *C. elegans*, which is part of a protein complex responsible for RNA interference (32), and the R2D2 protein of *Drosophila* (33), recently shown to be a DICER-associated protein. The RDE-4 protein, which seems to function only in short interfering RNA production, interacts with RDE-1 (Argonaute family), DICER, and a DexH box helicase. The *Drosophila* R2D2 protein facilitates short interfering RNA passage from DICER to the RNA-induced silencing complex. The HYL1 protein also contains two NLS sequences, and its C terminus comprises six almost perfect 28-aa repeats, a feature resembling the multiple 34-aa repeats in the *Chlamydomonas*

Abbreviations: miRNA, microRNA; PTGS, posttranscriptional gene silencing; dsRNA, double-stranded RNA; DCL1, DICER-LIKE 1, HEN1, HUA ENHANCER 1; LUC, luciferase; GUS, β-glucuronidase.

*To whom correspondence should be addressed. E-mail: nvf1@psu.edu.

Nac2 and Mbb1 proteins, which determine chloroplast transcript stability (34, 35). These observations prompted us to ask whether HYL1 is involved in miRNA or short interfering RNA production and function.

Here, we show that the accumulation of several miRNAs (miR159, -167, and -171) is depressed in *hyl1* mutant plants, as it is in *hen1-1* mutant plants, and elevated in plants overexpressing the HYL1 protein. Two of the three predicted target genes were expressed at higher levels in *hyl1* mutant plants than in wild-type plants, whereas all three were expressed at higher levels in *hen1-1* mutant plants. Transcripts of all three target genes were less abundant in plants expressing a *HYL1* cDNA from the strong cauliflower mosaic virus 35S promoter (35S::HYL1) than in wild-type plants, revealing an inverse relationship between HYL1 abundance and target transcript abundance. We show that transcripts of the miRNA target genes are more stable in *hyl1* mutant plants and less stable in HYL1 overexpressers than in wild-type plants after inhibition of RNA synthesis, but that dsRNA-mediated PTGS is unaffected in the *hyl1* mutant. We report that HYL1 protein is present both free and in a large ≈300-kDa complex. Using a GFP-HYL1 fusion, we show that HYL1 is predominantly in the nucleus, where it is commonly seen to be concentrated in small bodies and rings.

Materials and Methods

RNA Gel Blot Analysis. Total RNA was extracted from 1-month-old plants by using TRIzol (Invitrogen), and miRNAs were detected as described by Park *et al.* (14). Briefly, 50 μg of total RNA was fractionated on a denaturing 15% polyacrylamide gel containing 8 M urea, transferred to a Hybond N+ membrane (Amersham Biosciences) by using the Mini TransBlot electrophoretic transfer cell (Bio-Rad), and probed with ^{32}P-labeled antisense oligodeoxynucleotides (synthesized by Integrated DNA Technologies, Coralville, IA) for the miRNAs. The oligonucleotides were end-labeled with [γ-^{32}P]ATP by using T4 polynucleotide kinase. Hybridization was performed at 40°C by using Ultrahyb-oligo hybridization buffer (Ambion, Austin, TX).

For mRNA detection, 20 μg of total RNA was fractionated on a 1.2% agarose gel, transferred to a nylon membrane, and probed with PCR-amplified fragments of the target RNAs labeled with [α-^{32}P]dCTP by random priming. Hybridization was performed at 65°C as described (36). The *DCL1* transcript level was determined by RT-PCR as described below. Relative miRNA and predicted target mRNA levels were estimated by using NIH IMAGE (version 1.62) software to analyze data files obtained by using a phosphorimager. The RT-PCR results were quantified by using ALPHAIMAGER 2200 (version 5.1, AlphaEase) software. The measured miRNA and mRNA levels in *hyl1*, *hen1-1* (*hen1-1* seeds were the kind gift of Dr. Xuemei Chen, Rutgers University, Piscataway, NJ), and 35S::HYL1 plants were expressed as a fraction of the wild-type level. Membranes were stripped, checked by using a phosphorimager to ensure that stripping was complete, and then rehybridized with additional probes.

RNA Stability. One-month-old seedlings were transferred to small Petri dishes containing 5 ml of 1/2 MS medium containing or lacking 100 μg/ml cordycepin (3′-deoxyadenosine, Sigma), then harvested and frozen in liquid nitrogen at various intervals up to 12 h. Total RNA was extracted by using an Rneasy plant mini kit (Qiagen, Chatsworth, CA), quantified spectrophotometrically at 260 nm, and treated with DNase I according to the manufacturer's instructions (Invitrogen). First-strand cDNA synthesis was done by using 1–1.5 μg of total RNA; 1 μl of the first-strand cDNA was then used for PCR amplification in a reaction volume of 20 μl. PCRs were run for 25 cycles, which was determined in preliminary experiments by using 22, 25, and 29 cycles to be in the linear range for these cDNA concentrations. The following gene-specific primers were used for PCR amplification: ARF-8, 5′-CATGCTTGTGCTGGACCATT-3′ (forward) and 5′-CGCTTGGCACTGACAAAGAC-3′ (reverse); SCL6-III, 5′-GGGTTTCTTCTCGGATCCTC-3′ (forward) and 5′-AATCAGAGACGCCCATTGAC-3′ (reverse); MYB33, 5′-AAGAATTCTCGTCGCCTGAA-3′ (forward) and 5′-TCTCTCTGCCTTGGTGGAGT-3′ (reverse) and 5′-GAAGCTTCATCACCTCCATTG-3′ (forward); and ANP1, and 5′-TGATCACATTCTCTCCCAGTTG-3′ (reverse). The primers used to detect the DCL1 gene (nucleotides 5291–5691 of the coding sequence) were 5′-TTTTCATCGACGGTGTTCAA-3′ (forward) and 5′-CGCAGCTGAATCCTTAGCTT-3′ (reverse); these primers will detect both the full-length cDNA and its 2.5-kb cleavage product (37). Data from two to three amplifications of each gene were averaged and expressed as a fraction of the wild-type value (Fig. 1) or a percent of the maximum value (Fig. 2).

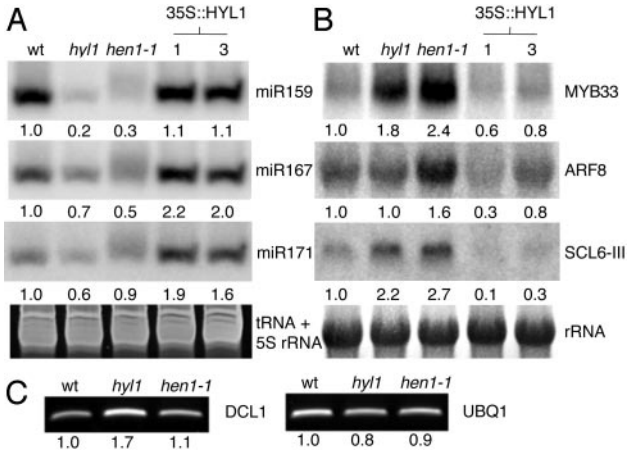

Fig. 1. miRNAs and predicted target mRNAs in 4-week-old wild-type, *hyl1*, *hen1-1*, and 35S::HYL1 plants (lanes 1 and 3 are from independent transformants). (*A*) RNA was fractionated on a denaturing 15% polyacrylamide gel, transferred to a membrane, and probed with ^{32}P-labeled antisense oligonucleotides for the indicated miRNAs. (*B*) RNA was fractionated on a 1.2% agarose gel, transferred to a nylon membrane, and probed with ^{32}P-labeled PCR-amplified fragments of the target RNAs indicated on the right. After hybridization and band quantification, the membranes used in *A* and *B* were stripped and rehybridized with additional probes. (*C*) RT-PCR analysis of *DCL1* expression in wild-type, *hyl1*, and *hen1-1* plants. The numbers below the blots are the ratio of the amount of the indicated RNA to the amount of RNA detected in wild-type plants.

Gene Silencing Assays. Luciferase (LUC) and β-glucuronidase (GUS) dsRNAs were prepared by using the HiScribe RNA interference transcription kit (New England Biolabs). DNA fragments ≈300 bp in length, containing coding sequences for the target genes, were amplified by using PCR with gene-specific primers (see below) and then cloned into LITMUS 28i vectors individually. The templates for *in vitro* transcription were amplified from the cloned inserts by PCR using a single T7 promoter-specific primer. The PCR products were purified by using a QIAquick PCR purification kit (Qiagen) and used for *in vitro* transcription. After *in vitro* transcription, the dsRNAs were annealed by incubation at 65°C for 5 min and cooling to room temperature. The annealed dsRNAs were quantified and analyzed in 1% TBE agarose gels. The following primers were used in the PCR: LUC, 5′-GAAGATCTCTCGCATGCCAGAGATCCTATT-3′ (forward) and 5′-AAGGCCTCCCCGACTTCCTTAGAGAG-3′ (reverse); GUS, 5′-GAAGATCTGGGCGAACAGTTCCTGATTA-3′ (forward) and 5′-AAGGCCTTTGACTGCCTCTTCGCT-3′ (reverse); T7, 5′-TAATACGACTCACTATAGG-3′.

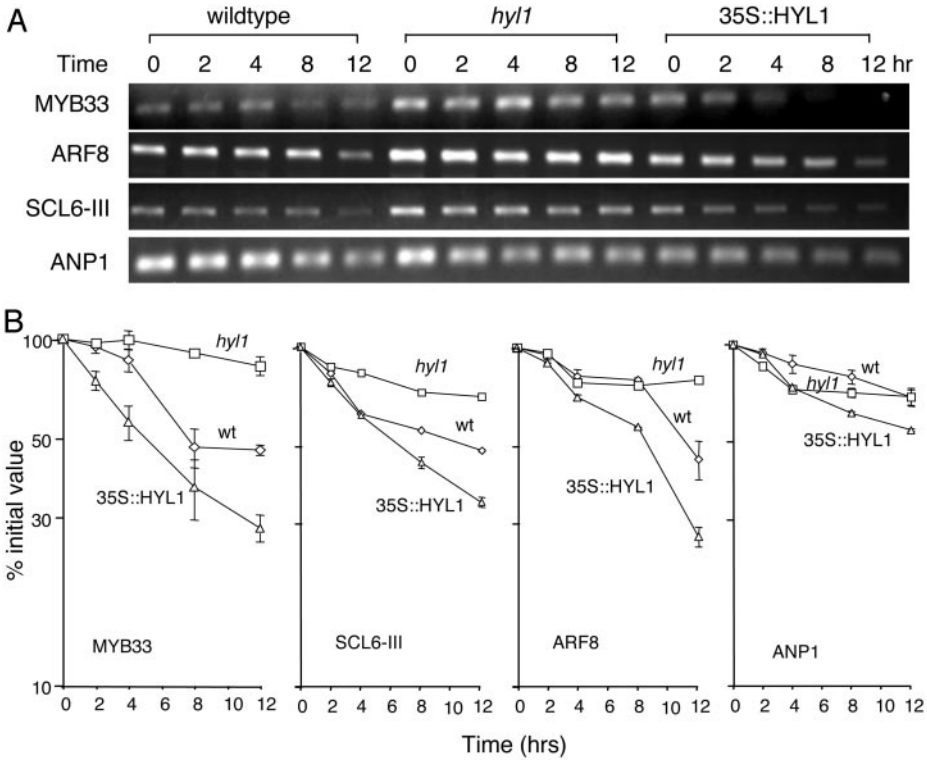

Fig. 2. Stability of target RNAs in wild-type, *hyl1*, and 35S::HYL1 (transformant 1 in Fig. 1) plants. (*A*) RT-PCR amplification of several target RNAs at various intervals after addition of 100 μg/ml cordycepin. (*B*) The results of several experiments such as those shown in *A* were quantified and plotted as a percentage of the initial value. Average values obtained with wild-type (wt) plants, *hyl1* mutants, and 35S::HYL1 overexpressers are represented by diamonds, squares, and triangles, respectively.

Protoplasts were isolated from wild-type and *hyl1* plants and transfected by a polyethylene glycol method as described by J. Sheen's laboratory (Harvard Medical School, Cambridge, MA; http://genetics.mgh.harvard.edu/sheenweb/protocols_reg.html). A volume of 200 μl of the protoplast suspension ($\approx$1–2 $\times$ 10^5 protoplasts per ml) was used for each transfection. For the gene silencing test, 15 μg of *LUC* or *GUS* dsRNA was cotransfected with the reporter plasmid containing a 35S::LUC and/or a 35S::GUS cDNA construct. The transfected protoplasts were incubated at 22°C for 12–16 h before collection and lysis. The LUC and GUS activities were measured by using the LUC assay system (Promega) and the Aurora TM GUS chemiluminescent reporter gene assay (ICN), respectively, by using a Sirius luminometer (Berthold, Nashua, NH).

HYL1-GFP Fusion Construct. The HYL1 gene was cloned from 35S::HYL1-GUS (30) by amplifying with the PCR primers 5′-GTCGACATGACCTCCACTGATGTTTC-3′ (forward) and 5′-CCATGG**CACCAGCACCAGCACCAGCACC**TGCGTGGCTTGCTTCT-3′ (reverse) (underlined sequences are the restriction sites used for cloning, and the boldfaced sequence indicates the spacer) to introduce a *Sal*I site at the 5′ end, remove the stop codon, and add a spacer followed by a *Nco*I site at 3′ end. The cloned HYL1 fragment was inserted into p4-eGFP vector (a kind gift from Simon Gilroy, Pennsylvania State University) at the N-terminal end of the GFP-coding sequence by using the *Sal*I and *Nco*I sites. The *HYL1-GFP* chimeric gene was expressed from the cauliflower mosaic virus 35S promoter. The 35S::HYL1-GFP fusion construct was transferred into the pCAMBIA3300 *Agrobacterium* binary vector and transformed into homozygous *hyl1* mutant plants. Transformed plants, identified by germinating seeds on 10 μg/ml glufosinate, had a wild-type phenotype, lacking the hyponastic leaves, short stature, and fertility abnormalities of the *hyl1* mutant, indicating that the HYL1-GFP fusion protein was able to complement the *hyl1* mutation.

Confocal Microscopy. *Arabidopsis* protoplasts were isolated as described above; $\approx$1.5 $\times$ 10^5 protoplasts were transfected with 50 μg of plasmid DNA (the total size of the plasmid was $\approx$5 kb) and incubated in the dark at 22°C for 16 h. GFP fluorescence was observed with an FV300 laser-scanning confocal microscope (Olympus, New Hyde Park, NY). GFP was excited with an argon ion laser (488 nm), and light was collected through a 510 long-pass and a 530 short-pass filter. Chloroplasts were excited with a green helium-neon laser with emission collected after filtering through a 565 long-pass filter. Images were taken at $\times$600 magnification, and FV300 software was used for analysis (version 4.0, Olympus). The experiments were repeated twice.

HYL1 Antibodies. A rabbit polyclonal antibody was raised (U.S. Biological, Swampscott, MA) against an internal repetitive peptide of 15 aa (N-CMSGLKEAAFGSVET-C, amino acids 400–414) predicted to be highly specific to HYL1.

Blue Native Gel Electrophoresis and Western Blotting. Blue native gel electrophoresis was performed by using a modification of the method described by Shagger *et al.* (38). Plant tissue was ground in liquid nitrogen and taken up in a buffer containing 20 mM Bis-Tris·HCl, pH 7.0, 50 mM ε-aminocaproic acid, 2 mM EDTA, 0.5% Triton X-100, and 10% glycerol. After centrifugation at 15,000 $\times$ *g* for 15 min, an aliquot of the supernatant was applied to a 5.5–16% polyacrylamide gradient gel containing 50 mM Bis-Tris·HCl (pH 7.0) and 50 mM ε-aminocaproic acid. The gel was run in blue cathode buffer (50 mM tricine/15 mM Bis-Tris·HCl, pH 7.0/0.02% Coomassie blue G 250) and anode

buffer (50 mM Bis-Tris·HCl, pH 7.0) at 200 V at 4°C. The high molecular weight calibration kit for native electrophoresis (Amersham Biosciences) was used for molecular weight estimation. After electrophoresis, proteins were transferred onto a Hybond-P poly(vinylidene difluoride) membrane (Amersham Biosciences). Immunoblotting was performed with rabbit polyclonal anti-HYL1 antibody (described above). After incubation with horseradish peroxidase-conjugated anti-rabbit IgG antibodies, proteins were visualized by using the ECL plus Western blotting detection reagents (Amersham Biosciences) under standard conditions.

Results and Discussion

HYL1 Affects miRNA and Target Transcript Levels. To determine whether miRNA levels are affected by the supply of HYL1 protein, we performed Northern blot hybridization analyses on several known miRNAs (miR159, miR167, and miR171) in RNA preparations from 1-month-old wild-type plants, *hyl1* and *hen1-1* mutants, and transgenic plants expressing an *HYL1* cDNA from a cauliflower mosaic virus 35S promoter. HYL1 protein was undetectable in homozygous *hyl1* plants and was ≈3-fold more abundant in 35S::HYL1 plants than in wild-type plants (data not shown). All three miRNAs tested were less abundant in both mutant plants and more abundant in 35S::HYL1 transgenic plants than in wild-type plants (Fig. 1*A*). To exclude the possibility that the low miRNA levels are an indirect effect of the *hyl1* mutation on expression of the *DCL1* gene (14), we used RT-PCR to check the *DCL1* gene expression level in the *hyl1* mutant. The *DCL1* transcript level, which is also controlled by an miRNA (37), is higher in the *hyl1* mutant than it is in either wild-type plants or *hen1-1* plants (Fig. 1*C*), indicating that the low miRNA levels are not attributable to misexpression of the *DCL1* gene.

The correlation between the levels of the miRNAs tested and HYL1 protein expression suggests that HYL1 is involved in miRNA metabolism. Because miRNAs can regulate gene expression by means of transcript destabilization, we first asked whether the HYL1 expression levels affect steady-state levels of predicted targets of the tested miRNAs. Those tested were auxin response factor 8 (At5g37020) for miR167, the Scarecrow-like gene SCL6-III (At3g60630) for miR171, and MYB33 (At5g06100) for miR159 (14, 39, 40). We used PCR-amplified cDNA fragments of each target gene to probe Northern blots prepared with mRNA isolated from wild-type plants, *hyl1* and *hen1-1* mutants, and 35S::HYL1 transgenic plants. All three of the predicted target genes were expressed at higher levels in the *hen1-1* mutant, and two of the three were expressed at higher levels in *hyl1* mutant than in wild-type plants (Fig. 1*B*). Moreover, transcripts of all three target genes were less abundant in 35S::HYL1 plants than in wild-type plants, implying an inverse relationship between the HYL1 level and the target transcript level.

Target RNA Stability. To determine whether the steady-state levels of target transcripts were a reflection of differences in their degradation rates, 4-week-old wild-type *hyl1* mutant and 35S::*HYL1* plants were treated with 100 μg/ml cordycepin to inhibit RNA synthesis, then collected at various times for RNA extraction and quantification of transcript levels by RT-PCR. Fig. 2*A* shows the results obtained for MYB33, ARF8, and SCL6-III miRNA targets, as well as ANP1, a mitogen-activated protein kinase kinase kinase gene that is not predicted to be miRNA-regulated. Results for the four genes are quantified and normalized for direct comparison in Fig. 2*B*. Consistent with Northern blot data, mRNA levels are higher in the *hyl1* mutant than in wild-type seedlings for the miRNA targets, but not the ANP1 mRNA. All of the mRNAs are degraded more slowly in *hyl1* mutants and more rapidly in 35S::HYL1 than in wild-type

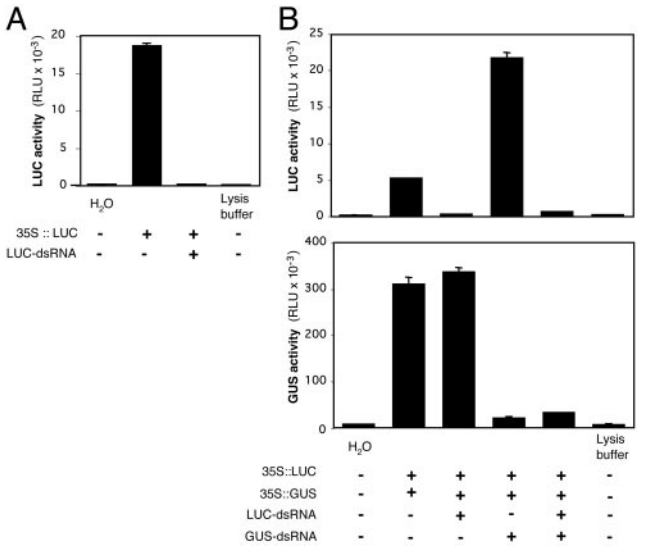

Fig. 3. PTGS in wild-type and *hyl1* protoplasts. (*A*) Protoplasts from wild-type plants were transfected with H_2O (mock-transfected), a 35S::LUC plasmid, and both the 35S::LUC and a LUC-dsRNA. After 12–16 h at 22°C, the transfected protoplasts were lysed, and LUC activity was measured (the lysis buffer was used as a control for the LUC assay). (*B*) The experiment was done by using *hyl1* protoplasts transfected with both 35S::LUC and 35S::GUS genes; the protoplasts were then subdivided, and the indicated dsRNAs were added to aliquots, which were then incubated and assayed for both activities.

seedlings, with the most marked differences detected for the MYB33 and SCL6-III genes. By contrast, ANP1mRNA is degraded relatively slowly and at comparable rates in mutant, wild-type, and 35S::HYL1 plants.

The mRNA decay curves seem to be biphasic in some cases, with an initial rapid degradation rate and a subsequent slower rate. Thus, for example, the initial rate is similar in wild-type, *hyl1*, and 35S::HYL1 plants but subsequently decreases in wild-type and *hyl1* plants. Moreover, it seems to decline sooner in the *hyl1* than in the wild-type plants. Although little is known about the quantitative relationships between miRNAs and their targets in plants, the present observations suggest that when RNA synthesis is interrupted by cordycepin, the supply of miRNA determines the initial decay rate until it is exhausted, after which the RNA decay rate reverts to a basal, non-miRNA rate. This is consistent with the results of recent studies on RhyB, a small bacterial regulatory RNA, which revealed a stoichiometric relationship between the regulatory RNA and its target with which it is degraded (4).

dsRNA-Mediated PTGS Is Not Compromised in the *hyl1* Mutant. To further inquire into the function of the HYL1 protein, we asked whether the dsRNA-mediated PTGS mechanism is affected by the *hyl1* mutation. The possibility that HYL1 is involved in PTGS is raised by the observation that RDE-4 and R2D2, the closest homologs of HYL1, are involved in RNA interference in *C. elegans* (32) and *Drosophila* (33), respectively. We asked whether the expression of two foreign genes, firefly LUC and a bacterial GUS gene expressed from the cauliflower mosaic virus 35S promoter, could be inhibited by homologous dsRNA. We transfected the plasmids carrying the 35S promoter-driven GUS and LUC genes into protoplasts prepared from wild-type and *hyl1* mutant *Arabidopsis* plants (41–43). We used *in vitro*-synthesized ≈300-nt dsRNAs corresponding to the coding sequence of the reporter gene to silence the transgenes. Fig. 3*A* shows that the LUC dsRNA effectively inhibits LUC expression of the cotransfected 35S::LUC gene, demonstrating that PTGS is triggered by

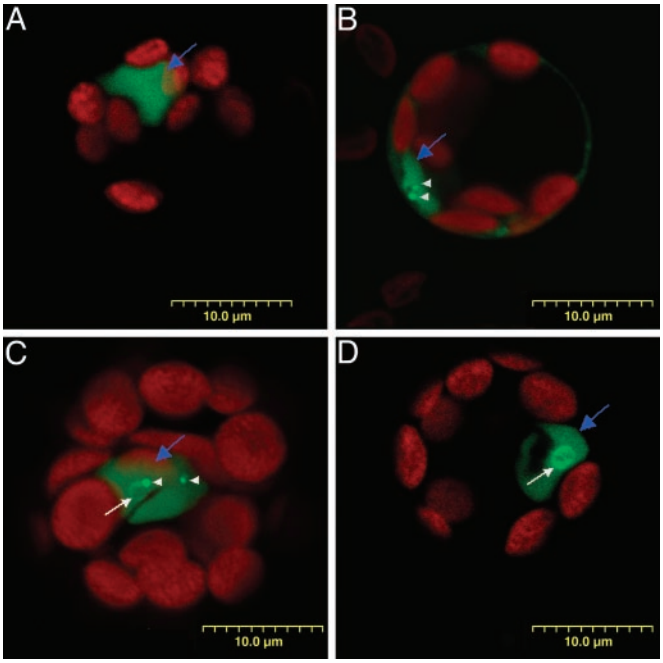

Fig. 4. Subcellular distribution of HYL1-GFP fluorescence. (*A*) Nuclear, uniform. (*B*) Nuclear and cytoplasmic. (*C*) Ring and bodies. (*D*) Ring. Blue arrows indicate the nucleus, white arrows designate HYL1-containing rings, and white arrowheads indicate the HYL1-containing nuclear bodies. The red structures are chloroplasts.

dsRNA in protoplasts. Similar experiments were carried out in *hyl1* protoplasts by using both 35S::LUC and a 35S::GUS plasmids and dsRNA homologous to each. The homologous dsRNA inhibited gene expression in mutant protoplasts, whereas the heterologous dsRNA did not (Fig. 3*B*). Thus, sequence-specific PTGS by dsRNA is not compromised by the *hyl1* mutation. It remains to be determined whether the *hyl1* mutation affects other aspects of PTGS (44).

Subcellular Distribution of HYL1. We previously reported that HYL1 concentrates in the nucleus of transfected onion epidermal cells (30). To gain further insight into the subcellular distribution of the HYL1 protein, we made a HYL1-GFP translational fusion and used confocal microscopy to analyze *Arabidopsis* protoplasts expressing the HYL1-GFP protein. The fusion protein was shown to be functional by stably transforming the fusion construct into *hyl1* mutant plants and showing that it rescues the mutant phenotype (data not shown). Although HYL1 is concentrated in the nucleus in most cells, in some cells it is also observed in the cytoplasm, where it has a somewhat patchy distribution (Fig. 4 *A* and *B*). Among 28 protoplasts analyzed in detail, 22 showed fluorescence only in nuclei, whereas the remaining 6 exhibited fluorescence in both nucleus and cytoplasm. Within the nucleus, the HYL1-GFP fusion protein is frequently observed to concentrate in two subnuclear structures: small bodies and rings. Most of the small nuclear bodies had diameters $\leq$0.7 μm, but a few were 1.0 μm in diameter or even larger (Fig. 4 *B* and *C*). Ring-like structures usually had diameters of $\geq$2.0 μm (Fig. 4 *C* and *D*). Among the 20 protoplasts with subnuclear structures, 6 contained rings and 15 contained subnuclear bodies. One of these cells had both a ring and several small bodies (Fig. 4*C*). It should also be noted that although HYL-GFP fluorescence was occasionally observed to be cytoplasmic in all three of the transfections experiments, the cytoplasmic distribution of HYL1-GFP fluorescence differed from that of GFP controls, giving a rather patchy appearance (Fig. 4*B*) in contrast to the uniform cytoplasmic fluorescence observed with GFP controls (data not shown).

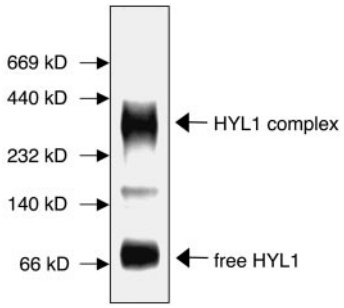

Fig. 5. Blue native gel electrophoretic analysis of HYL1. Total protein extract from wild-type plants was fractionated as described in *Materials and Methods*, transferred to a poly(vinylidene difluoride) membrane, and probed with anti-HYL1 antibody.

To determine whether HYL1 is in macromolecular complexes, we analyzed protein extracts of wild-type cells by using blue native gel electrophoresis (Fig. 5 and ref. 38). When the complexes were further resolved in a denaturing gel (data not shown), HYL1 was detected in the $\approx$300-kDa complex, as well as in the major band migrating somewhat more slowly than the 66-kDa marker. These correspond to complexed and free HYL1, respectively, and one-third to one-half of the immunologically detectable HYL1 protein was in the complex. A minor band detected with anti-HYL1 antibody migrating slightly more slowly than the 140-kDa marker on the blue native gel did not contain a protein that comigrates with HYL1 on the denaturing gel and hence is attributable to an immunologically crossreacting protein. A similar distribution of free and complexed proteins has been detected by gel filtration chromatography (data not shown). Thus, about one-half of the HYL1 protein is present in a high molecular weight complex, whereas the remainder appears to be free.

In summary, we have presented evidence that the supply of HYL1 dsRNA-binding protein affects the abundance of several miRNAs and their predicted target RNAs. The stability of the target RNA is inversely proportional to the level of *HYL1* gene expression, whereas the abundance of the corresponding miRNA is directly correlated with *HYL1* gene expression and protein abundance, although some residual miRNA was detected in the *hyl1* null mutant for all of the sequences tested. Differences in the HYL1 protein level affect miRNA metabolism and mRNA stability but not dsRNA-mediated PTGS. HYL1 is predominantly a nuclear protein and is detected in nuclear bodies and ring-like structures reminiscent of Cajal or coiled bodies, known to be involved in nuclear RNA processing in association with the nucleolus (45, 46). One-third to one-half of the HYL1 protein in crude extracts is in the form of an $\approx$300-kDa complex. These observations imply that the HYL1 protein is in a macromolecular complex involved in miRNA metabolism and further suggest that some aspects of miRNA metabolism occurs in the nucleus, possibly in association with perinucleolar RNA-processing bodies. Studies are underway to determine the nature of the nuclear HYL1-containing rings and bodies.

Because the levels of several different miRNAs and their target RNAs are affected by the expression level of the *HYL1* gene, albeit to different extents, the HYL1 protein seems to be involved in a common aspect of miRNA metabolism. The fact that miRNAs are present at low levels in the null *hyl1* mutant suggests that the protein is not essential for miRNA biogenesis. Although this may be attributable to redundancy or degeneracy in the constituents of the miRNA processing machinery, another

possibility is that HYL1 regulates the stability of a processing or degradation intermediate. This is supported by the observation that target mRNA stability can be substantially reduced in the HYL1 overexpresser even when the miRNA level is not markedly enhanced (Fig. 1, miR159).

The *hyl1* mutant exhibits a number of developmental abnormalities, many of which are associated with underlying defects in hormonal signaling or responses (30, 31). Rapid, transient increases in transcript levels are a common early response to changes in hormone levels (47–49). The SCL6-III, ARF8, and MYB33 are all proteins that are either known or likely transcriptional regulators mediating hormone responses (22, 50, 51). It was recently reported that although overexpression of the MYB33 gene itself had no discernible phenotypic effect, overexpression of a gene mutated to reduce homology to miR159 gave plants that have the hyponastic leaf phenotype from which the *hyl1* mutant derives its name (7, 30), implying that the developmental abnormality results not from overexpression of the gene but from inability to degrade the mRNA. The results of the present studies suggest that miRNA-mediated regulation of mRNA stability may be as important a regulatory mechanism in the rapid, hormone-induced changes in transcript levels as protein destabilization (52).

We thank Drs. Patrick Masson, Thoru Pederson, and Vicki Vance for many helpful suggestions on the manuscript. This work was supported by National Science Foundation Grant IBN 00-91650.

1. Weiner, A. (2003) *Mol. Cell* **12,** 535–536.
2. Wassenegger, M. (2002) *Int. Rev. Cytol.* **219,** 61–113.
3. Bernstein, E., Denli, A. M. & Hannon, G. J. (2001) *RNA* **7,** 1509–1521.
4. Masse, E., Escorcia, F. E. & Gottesman, S. (2003) *Genes Dev.* **17,** 2374–2383.
5. Zeng, Y., Yi, R. & Cullen, B. R. (2003) *Proc. Natl. Acad. Sci. USA* **100,** 9779–9784.
6. Lagos-Quintana, M., Rauhut, R., Lendeckel, W. & Tuschl, T. (2001) *Science* **294,** 853–858.
7. Palatnik, J. F., Allen, E., Wu, X., Schommer, C., Schwab, R., Carrington, J. C. & Weigel, D. (2003) *Nature* **425,** 257–263.
8. Aukerman, M. J. & Sakai, H. (2003) *Plant Cell* **15,** 2730–2741.
9. Lagos-Quintana, M., Rauhut, R., Yalcin, A., Meyer, J., Lendeckel, W. & Tuschl, T. (2002) *Curr. Biol.* **12,** 735–739.
10. Lau, N. C., Lim, L. P., Weinstein, E. G. & Bartel, D. P. (2001) *Science* **294,** 858–862.
11. Lee, R. C. & Ambros, V. (2001) *Science* **294,** 862–864.
12. Llave, C., Kasschau, K. D., Rector, M. A. & Carrington, J. C. (2002) *Plant Cell* **14,** 1605–1619.
13. Mourelatos, Z., Dostie, J., Paushkin, S., Sharma, A., Charroux, B., Abel, L., Rappsilber, J., Mann, M. & Dreyfuss, G. (2002) *Genes Dev.* **16,** 720–728.
14. Park, W., Li, J., Song, R., Messing, J. & Chen, X. (2002) *Curr. Biol.* **12,** 1484–1495.
15. Reinhart, B. J., Weinstein, E. G., Rhoades, M. W., Bartel, B. & Bartel, D. P. (2002) *Genes Dev.* **16,** 1616–1626.
16. Jacobsen, S. E., Running, M. P. & Meyerowitz, E. M. (1999) *Development (Cambridge, U.K.)* **126,** 5231–5243.
17. Grishok, A., Pasquinelli, A. E., Conte, D., Li, N., Parrish, S., Ha, I., Baillie, D. L., Fire, A., Ruvkun, G. & Mello, C. C. (2001) *Cell* **106,** 23–34.
18. Hutvagner, G. & Zamore, P. D. (2002) *Science* **297,** 2056–2060.
19. Schauer, S. E., Jacobsen, S. E., Meinke, D. W. & Ray, A. (2002) *Trends Plant Sci.* **7,** 487–491.
20. Lee, Y., Ahn, C., Han, J., Choi, H., Kim, J., Yim, J., Lee, J., Provost, P., Radmark, O., Kim, S. & Kim, V. N. (2003) *Nature* **425,** 415–419.
21. Boutet, S., Vazquez, F., Liu, J., Beclin, C., Fagard, M., Gratias, A., Morel, J. B., Crete, P., Chen, X. & Vaucheret, H. (2003) *Curr. Biol.* **13,** 843–848.
22. Llave, C., Xie, Z., Kasschau, K. D. & Carrington, J. C. (2002) *Science* **297,** 2053–2056.
23. Chen, X. (September 11, 2003) *Science, 10.1126/science.1088060.*
24. Doench, J. G., Petersen, C. P. & Sharp, P. A. (2003) *Genes Dev.* **17,** 438–442.
25. Lee, R. C., Feinbaum, R. L. & Ambros, V. (1993) *Cell* **75,** 843–854.
26. Wightman, B., Ha, I. & Ruvkun, G. (1993) *Cell* **75,** 855–862.
27. Reinhart, B. J., Slack, F. J., Basson, M., Pasquinelli, A. E., Bettinger, J. C., Rougvie, A. E., Horvitz, H. R. & Ruvkun, G. (2000) *Nature* **403,** 901–906.
28. Krichevsky, A. M., King, K. S., Donahue, C. P., Khrapko, K. & Kosik, K. S. (2003) *RNA* **9,** 1274–1281.
29. Kasschau, K. D., Xie, Z., Allen, E., Llave, C., Chapman, E. J., Krizan, K. A. & Carrington, J. C. (2003) *Dev. Cell* **4,** 205–217.
30. Lu, C. & Fedoroff, N. (2000) *Plant Cell* **12,** 2351–2366.
31. Lu, C., Han, M. H., Guevara-Garcia, A. & Fedoroff, N. V. (2002) *Proc. Natl. Acad. Sci. USA* **99,** 15812–15817.
32. Tabara, H., Yigit, E., Siomi, H. & Mello, C. C. (2002) *Cell* **109,** 861–871.
33. Liu, Q., Rand, T. A., Kalidas, S., Du, F., Kim, H. E., Smith, D. P. & Wang, X. (2003) *Science* **301,** 1921–1925.
34. Vaistij, F. E., Boudreau, E., Lemaire, S. D., Goldschmidt-Clermont, M. & Rochaix, J. D. (2000) *Proc. Natl. Acad. Sci. USA* **97,** 14813–14818.
35. Boudreau, E., Nickelsen, J., Lemaire, S. D., Ossenbuhl, F. & Rochaix, J. D. (2000) *EMBO J.* **19,** 3366–3376.
36. Tsugeki, R., Kochieva, E. Z. & Fedoroff, N. V. (1996) *Plant J.* **10,** 479–489.
37. Xie, Z., Kasschau, K. D. & Carrington, J. C. (2003) *Curr. Biol.* **13,** 784–789.
38. Schagger, H., Cramer, W. A. & von Jagow, G. (1994) *Anal. Biochem.* **217,** 220–230.
39. Rhoades, M. W., Reinhart, B. J., Lim, L. P., Burge, C. B., Bartel, B. & Bartel, D. P. (2002) *Cell* **110,** 513–520.
40. Bartel, B. & Bartel, D. P. (2003) *Plant Physiol.* **132,** 709–717.
41. Sheen, J. (2001) *Plant Physiol.* **127,** 1466–1475.
42. Abel, S. & Theologis, A. (1998) *Methods Mol. Biol.* **82,** 209–217.
43. Kovtun, Y., Chiu, W. L., Tena, G. & Sheen, J. (2000) *Proc. Natl. Acad. Sci. USA* **97,** 2940–2945.
44. Beclin, C., Boutet, S., Waterhouse, P. & Vaucheret, H. (2002) *Curr. Biol.* **12,** 684–688.
45. Gall, J. G. (2000) *Annu. Rev. Cell Dev. Biol.* **16,** 273–300.
46. Boudonck, K., Dolan, L. & Shaw, P. J. (1999) *Mol. Biol. Cell* **10,** 2297–2307.
47. Gil, P. & Green, P. J. (1996) *EMBO J.* **15,** 1678–1686.
48. Kuhn, J. M. & Schroeder, J. I. (2003) *Curr. Opin. Plant Biol.* **6,** 463–469.
49. Fedoroff, N. V. (2002) *Curr. Opin. Plant Biol.* **5,** 452–459.
50. Gocal, G. F., Sheldon, C. C., Gubler, F., Moritz, T., Bagnall, D. J., MacMillan, C. P., Li, S. F., Parish, R. W., Dennis, E. S., Weigel, D. & King, R. W. (2001) *Plant Physiol.* **127,** 1682–1693.
51. Tiwari, S. B., Hagen, G. & Guilfoyle, T. (2003) *Plant Cell* **15,** 533–543.
52. Leyser, O. (2001) *Curr. Opin. Plant Biol.* **4,** 382–386.